

Study on mechanical and tribological behavior of cenosphere filled vinylester composites – A Taguchi method

Sunil Thakur* & S R Chauhan

Department of Mechanical Engineering, National Institute of Technology, Hamirpur 177 005, India

Received 16 October 2012; accepted 2 May 2013

The wear behaviour of vinylester composites filled with uniform sized sub-micron cenosphere particle is discussed in this paper. Three distinct sizes of uniform sized cenosphere particles (dia: 2 μm , 900 nm and 400 nm) are prepared in our laboratory and used as model fillers in composites. The experiments have been carried on a pin on disc arrangement at normal temperature conditions. The influence of friction and wear parameters like normal load, speed, sliding distance and filler content on the friction and wear rate has been investigated. In this study, a plan of experiments, based on the techniques of Taguchi, is performed to acquire data in a controlled way. An orthogonal array $L_{27}(3^{13})$ and analysis of variance (ANOVA) are applied to investigate the influence of process parameters on the coefficient of friction and sliding wear behaviour of these composites. The tensile, flexural and compressive strength of the vinylester composites are determined on a universal materials testing machine. It is found that the submicron size particulates as the fillers contributed significantly to improve the mechanical properties and wear resistance of the vinylester composites. The wear mechanisms are studied by scanning electron microscopy.

Keywords: Composites, Cenosphere, Friction, Taguchi method, Tribology, Vinylester resin, Wear

Polymer and polymer matrix composites have been finding great potentials in the industry as a class of important triboengineering materials. High performance polymer composite materials are used increasingly for engineering applications under working condition¹⁻³. The materials must provide unique mechanical and tribological properties combined with a low specific weight and a high resistance to degradation in order to ensure safety and economic efficiency. Composite materials have replaced metals in various engineering applications owing to their numerous advantages like high strength-to-weight ratio, low cost⁴⁻⁶. There is always an increasing demand for use of these materials in defense applications like naval ships, warplanes, armored vehicles and sea vehicles. In production industry polymer and their composites are being increasingly employed in view of their good strength and low densities. Polymer composites have been used successfully for many decades as engineering materials. Polymer composites are the most rapidly growing class of materials due to their combination of high specific strength and specific modulus. They have been designed and manufactured for various applications such as aircraft, automobiles and civil structure⁷⁻⁹. A number of matrix materials are available, including carbon, ceramics, glasses, metals and polymers. The primary

means of improving engine efficiency are to take advantage of the high specific stiffness and strength of composites for weight reduction¹⁰⁻¹². Polymer composites exhibit excellent friction and wear characteristics even without external activations and can provide maintenance free operation, excellent corrosion resistance.

Inorganic particulate filled vinylester matrix composites have been extensively studied during the last two decades due to their increasing applications in coatings, electronic packaging and dental restoratives¹³⁻¹⁶. The particles in these composites are generally of micrometer size. Use of nanoparticles as fillers in vinylester matrix composites is nowadays attracting a great deal of attention from materials scientists, technologists and industrialists¹⁷⁻¹⁹. These new nanocomposite systems could have broader application potentials with their unique optical, electrical and magnetic properties. The success of their technical applications depends to a large extent on a better understanding of both the nature of the nanocomposites and the relationship between structures, properties and processing. Obviously, their mechanical response is essential to the understanding. In particular, an understanding of the wear properties of the composites is important in some applications. The understanding of the wear behavior of inorganic nanoparticle filled vinylester matrix composites are still very limited²⁰⁻²². The wear

*Corresponding author (E-mail: sunilthakur.nith@gmail.com)

resistance of the nanocomposites might be decreased or increased depending on the type of particles, particle size and size distribution, interfacial actions between particle and matrix resin, particle content and state of dispersion of the particles in the composites.

The Taguchi technique is a powerful tool for the design of high quality systems²³. The Taguchi approach to experimentation provides an orderly way to collect, analyze and interpret data to satisfy the objectives of the study. In the design of experiments, one can obtain the maximum amount of information for the amount of experimentation. Taguchi parameter design can optimize the performance characteristics through the setting of design parameters and reduce the sensitivity of the system performance to the source of variation²⁴⁻²⁶. This technique is a powerful tool for acquiring the data in a controlled way and to analyze the influence of process parameters over some specific parameters, which is an unknown function of these process variables. The Taguchi technique creates a standard orthogonal array to consider the effect of several factors on the target value and defines the plan of experiments. The experimental results are analyzed by using analysis of means and variance of the influence of factors²⁷.

The present research work is planned for developing light weight cenosphere particulates filled vinylester composites and to understand the tribological characteristics of these composites under dry sliding conditions. The objectives of this work are to investigate the effects of particle size, applied normal loads and sliding speed on the tribological characteristics of cenosphere filled vinylester composites. Three distinct sizes of cenosphere particulates 2 μm , 900 nm and 400 nm have been used as model fillers for preparation of vinylester composites. Wear tests using a pin-on-disc setup were carried out and the wear mechanisms were studied by scanning electron microscope (SEM) observations. This work will contribute to the better understanding of the micron and submicron size filled vinylester composites which are fundamental in their applications. Cenosphere is to be used in polymer composites as a low cost material for structural materials.

Experimental Procedure

Materials

Vinylester resin is the matrix material used for the present investigations. The type of resin used in this work is vinylester resin (density 1.23 g/cm³) supplied by Northan Polymer Ltd., Delhi, India and the Cenosphere

(hardness 5-6 MOH, density 0.4-0.6 g/cm³) supplied by Cenosphere India Pvt. Ltd. Vinylester is a hybrid form of polyester resin which has been toughened with epoxy molecules within the main molecular structure. Vinylester resins are stronger than polyester resins and cheaper than epoxy resins. The filler material used in this study is cenosphere. Cenospheres are inert hollow silicate spheres. The shape of cenosphere is spherical and the color is light gray.

Composite fabrication

The filler material, i.e., the cenosphere of three different size (2 μm , 900 nm and 400 nm) mixed with vinylester resin (10wt%) by conventional hand-lay-up technique and slowly poured in glass tubes so as to get cylindrical specimens (diameter 12 mm, length 120 mm). Also 1.5% of cobalt naphthalate (as accelerator) and 1.5% of methyl-ethyl-ketone-peroxide (MEKP) as the hardener is mixed thoroughly in composite materials. The mixer is stirred mechanically to disperse the filler particles in the composites. The composites are poured into the glass tube and then the glass tube was kept for post-curing at room temperature for 24 h. The hardened composite samples are extracted from the glass tube. Specimens of suitable dimension are cut using a diamond cutter for coefficient of friction test and specific wear test.

Friction and wear measurements

The friction and sliding wear performance evaluation of vinylester and its composites C₁, C₂ and C₃ under dry sliding conditions were carried out on a pin-on-disc type friction and wear monitoring test rig (DUCOM) as per ASTM G 99. During the test, friction force was measured by a transducer mounted on the loading arm. The friction force readings are taken as the average of 100 readings every 40 s for the required period. For this purpose a microprocessor controlled data acquisition system is used. The environmental condition in the laboratory was 23°C and 43% relative humidity. Weight loss method was used for finding the specific wear. For each condition, at least two tests were performed and the mean value of weight loss was reported. During these experiments initial and final weights of the specimens were measured. The material loss from the composite surface is measured using a precision electronic balance with accuracy ± 0.01 mg. Figure 1 shows the photograph of wear and friction monitor. The specific wear rate (mm³/Nm) is then expressed on 'volume loss' bases:

$$K_s = \frac{\Delta M}{\rho L F_n} \quad \dots (1)$$

Where K_s is the specific wear rate (mm^3/Nm), ΔM is the mass loss in the test duration (g), ρ is the density of the composite (g/cm^3), F_n is the applied normal load (N) and L is the total sliding distance (m).

Experimental design

The Taguchi method is a commonly adopted approach for optimizing design parameters. The method is originally proposed as a means of improving the quality of products through the application of statistical and engineering concepts. Since experimental procedures are generally expensive and time consuming, the need to satisfy the design objectives with the least number of tests is clearly an important requirement. Table 1 shows the factors to be studied and the assignment of the corresponding levels. The array chosen was the L27 (3^{13}) which has 27 rows corresponding to the number of tests (20 degrees of freedom) with 13 columns at three levels, as shown in Fig. 2 the factors and the interactions are assigned to the columns. The tests are conducted at room temperature as per experimental design given in Table 3, each column represents a test parameter whereas a row stands for a treatment or test condition which is nothing but a combination of parameter levels. In the full factorial experiment design, it would require $3^5=243$ runs to study five parameters each at three levels whereas, the Taguchi factorial experiment approach reduces it to only 27 runs offering a great advantage in term of experimental time and cost.

The plan of the experiments is as follows: the first column is assigned to load (A), the second column to filler content (B), the fifth column to roughness (C)



Fig. 1 — Photograph of wear and friction monitor

and the ninth column to speed (D), the tenth column to sliding distance (E) the third and fourth column are assigned to $(A \times B)_1$ and $(A \times B)_2$ respectively to estimate interaction between load (A) and filler content (B), the sixth and seventh column are assigned to $(B \times C)_1$ and $(B \times C)_2$ respectively to estimate the interaction between filler content (B) and roughness (C), the eighth and eleventh column are assigned to $(A \times C)_1$ and $(A \times C)_2$ respectively to estimate interaction between the load (A) and roughness (E) and the remaining columns are used to estimate experimental errors. The output to be studied is coefficient of friction (COF) and specific wear rate (W_s).

Mechanical characteristics

The experimental density of the composites is obtained by the Archimedes principle of weighing small pieces cut from the large composite panel first in the air and then in water. Theoretical density of the composite is calculated and compared with experimental density in order to calculate the void fraction of the composites. Hardness measurement is done using a Rockwell-hardness tester according to ASTM D785-89 equipped with a steel ball indenter (1/16") indenter by applying a load of 100 kgf and the average value of six tests is taken. The tensile test is generally performed on rectangular flat composite specimens as per ASTM D 3039-76 test standards on a universal testing machine (UTM) Hounsfield H25KS. The flexural and compressive strength tests are conducted as per ASTM standard D790 using the same UTM.

Table 1 — Levels of variables used in the experiments

Factor	Level			Units
	I	II	III	
A: Load	10	40	70	N
B: Filler content	2	0.9	0.4	μm
C: Roughness	0.02	0.2	0.7	μm
D: Speed	300	600	900	rpm
E: Sliding distance	2000	4000	6000	m

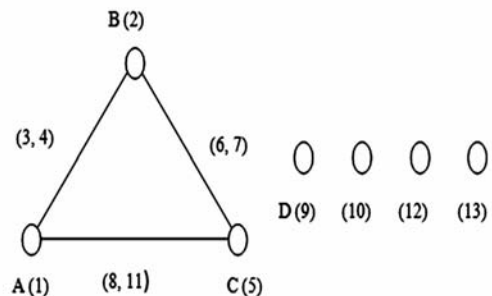


Fig. 2 — Linear graph for L27

Surface morphology

The surface morphologies of cenosphere filled vinylester composites have been investigated using scanning electron microscopy (SEM) on an FEI quanta FEG 450 electron microscope to analyze the associated worn surface and structural integrity of such multiphase micro-composite materials. The surfaces of the specimens were gold sputter coated prior to examination to make the surfaces conductive.

Results and Discussion

Mechanical properties of vinylester composites

The theoretical and measured densities along with the corresponding volume fraction of voids are presented in Table 2. The composites under investigation consists of two components namely matrix and particulate filler. Hence density of composites can be calculated using rule-of-mixture as shown in the following expression:

$$\rho_t = \frac{1}{\left(\frac{W_m}{\rho_m}\right) + \left(\frac{W_p}{\rho_p}\right)} \quad \dots (2)$$

Where W and ρ represent the weight fraction and density. The suffix m , p and t stand for the matrix, particulate filler and the composite materials respectively. The actual density (ρ_s) of the composites can be determined experimentally by simple water immersion technique. The volume fraction of the voids (V_v) in the composites is calculated using Eq. (3).

$$V_v = \frac{(\rho_t - \rho_e)}{\rho_t} \quad \dots (3)$$

It is clear from Table 2 that increasing amount of porosity is observed with increasing the volume fraction especially for small particle sizes of composites. In this work, smaller particle size vinylester composites show higher void fraction than large particle composites as void fraction also depends on fabrication techniques. This may be due to the fact that composite material

Table 2 — Material and test condition

Samples	Composites specification	Experimental density (g/cm ³)	Theoretical density (g/cm ³)	Voids fraction (%)
C ₁	2 μm cenosphere + vinylester	1.0776	1.1229	4.0342
C ₂	900 nm cenosphere + vinylester	1.0531	1.1229	6.2160
C ₃	400 nm cenosphere + vinylester	1.0215	1.1229	9.0302

which may entrap air during the preparation of composite samples in hand layup technique. It is believed to achieve an improvement of the bonding between the submicron size particle and matrix.

The variation in the hardness of vinylester composites is shown in Fig. 3(a). It can be observed from the figure that the hardness of the vinylester composites is

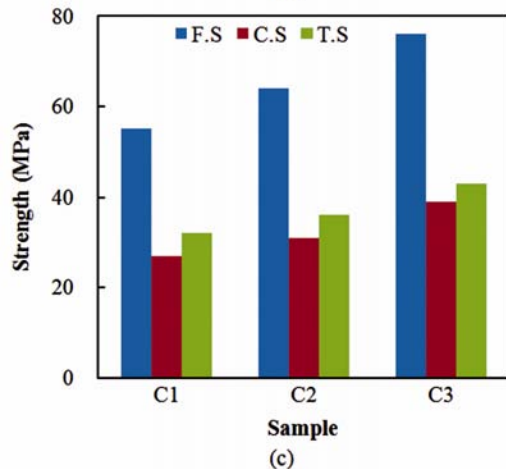
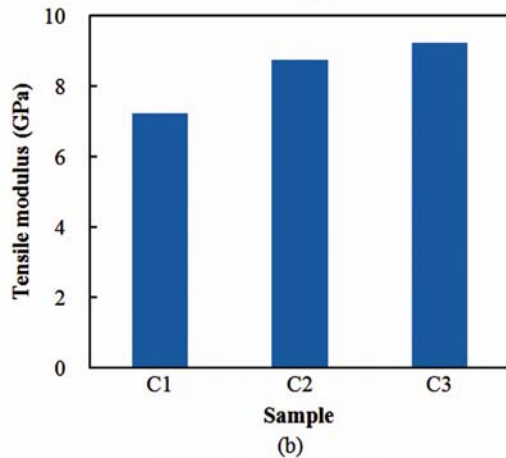
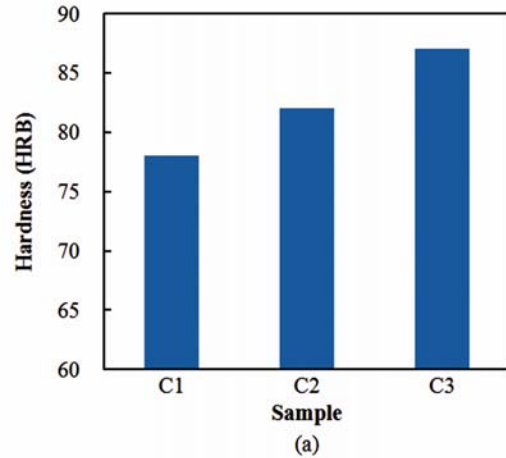


Fig.3 — Strength and hardness comparison of composite sample

improved and this improvement is a function of the cenosphere particle size. Among all the composites under this investigation, the composites reinforced with 2 μm 900 nm and 400 nm respectively, the value 78, 82 and 87 HRB. This is possible only if the interface between the matrix and filler is stronger. The variation of tensile strength, compressive and flexural strengths of vinylester composites with cenosphere content is presented in Fig. 3(b). The tensile strength refers to the combined strength and bonding energy between filler and the matrix. Little improvement in tensile strength for the vinylester composites is observed when the cenosphere content has decreased particle size. The above changes occur due to the interaction of cenosphere and matrix is good, it also depends on size of particle. The compressive strength of the vinylester composites reinforced with 2 μm , 900 nm and 400 nm respectively is 27, 31 and 39 MPa. The higher compressive strength it means matrix bear the maximum load, the strength depends on matrix strength, type of filler content. The small size particle interaction with the matrix is good as compared to the large size particle. Figure 3(c) shows the variation of flexural strength of vinylester composites with different particle size. Under

a flexural loading situation a gradual improvement in flexural strength with the particle size reduces is noticed in composites. The flexural strength of 400 nm cenosphere filled vinylester composite is higher as compared to 900 nm cenosphere filled vinylester composite. The above changes which are happening in flexural strength due to the poor bonding action, the poor bonding action in large size particle composite than the small size particle composite.

Analysis of experimental results

The experimental data for coefficient of friction and specific wear rate are given in Table 3. The data reported is the average of two replications. From Table 3 the overall mean for the S/N ratio of the coefficient of friction and the specific wear rate are found to be 4.6144 db and 87.3644 db respectively. The analyses of the experimental data are carried using the software MINITAB 16 specially used for the design of experimental applications. Before analyzing the experimental data using this method for predicting the measure of performance, the possible interactions between control factors are considered. This factorial design incorporates a simple means of testing for the presence of the interaction effects.

Table 3 — Experimental design using L_{27} array

RUN	Load (N)	Filler content (μm)	Roughness (μm)	Speed (rpm)	Sliding distance (m)	COF (μ)	S/N Ratios (dB)	Specific wear rate (mm^3/Nm)	S/N Ratios (dB)
1	10	2	0.02	300	2000	0.73	2.73354	0.000055	85.1927
1	10	2	0.2	600	4000	0.71	2.97483	0.000058	84.7314
2	10	2	0.7	900	6000	0.68	3.34982	0.000064	83.8764
3	10	900	0.02	600	4000	0.68	3.34982	0.000053	85.51448
4	10	900	0.2	900	6000	0.74	2.61536	0.000057	84.88250
5	10	900	0.7	300	2000	0.69	3.22301	0.000063	84.01318
6	10	400	0.02	900	6000	0.64	3.87640	0.000052	85.67993
7	10	400	0.2	300	2000	0.66	3.60912	0.000056	85.03623
8	10	400	0.7	600	4000	0.7	3.09803	0.000058	84.7314
9	40	2	0.02	600	6000	0.67	3.47850	0.00006	84.43695
10	40	2	0.2	900	2000	0.69	3.22301	0.000059	84.58296
11	40	2	0.7	300	4000	0.75	2.49877	0.000061	84.29340
12	40	900	0.02	900	2000	0.55	5.19274	0.000059	84.58296
13	40	900	0.2	300	4000	0.57	4.88250	0.000058	84.73144
14	40	900	0.7	600	6000	0.64	3.87640	0.00006	84.43697
15	40	400	0.02	300	4000	0.52	5.67993	0.000035	89.11863
16	40	400	0.2	600	6000	0.59	4.58295	0.000039	88.17870
17	40	400	0.7	900	2000	0.63	4.01318	0.000045	86.9357
18	70	2	0.02	900	4000	0.5	6.02059	0.00003	90.45755
19	70	2	0.2	300	6000	0.53	5.51448	0.000033	89.62971
20	70	2	0.7	600	2000	0.56	5.03623	0.000029	90.7524
21	70	900	0.02	300	6000	0.46	6.74484	0.000025	92.0412
22	70	900	0.2	600	2000	0.49	6.19607	0.000028	91.0569
23	70	900	0.7	900	4000	0.49	6.19607	0.000026	91.7005
24	70	400	0.02	600	2000	0.42	7.53501	0.000019	94.4249
25	70	400	0.2	900	4000	0.4	7.95880	0.000023	92.76543
26	70	400	0.7	300	6000	0.44	7.13094	0.000028	91.05689

Figures 4 and 6 shows graphically the effect of the five control factors of coefficient of friction and specific wear rate of the specimens C₁, C₂ and C₃. The analysis of results gives the combination factors resulting in minimum coefficient of friction and

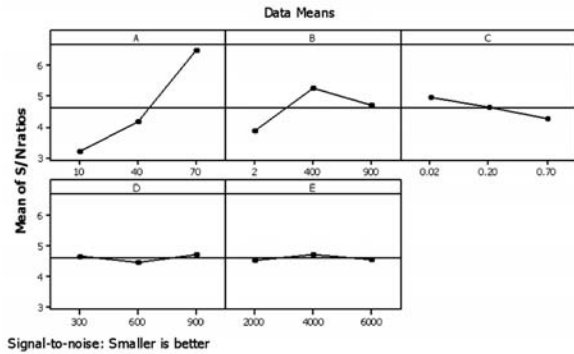


Fig. 4 — Main effect plot for S/N ratios for COF

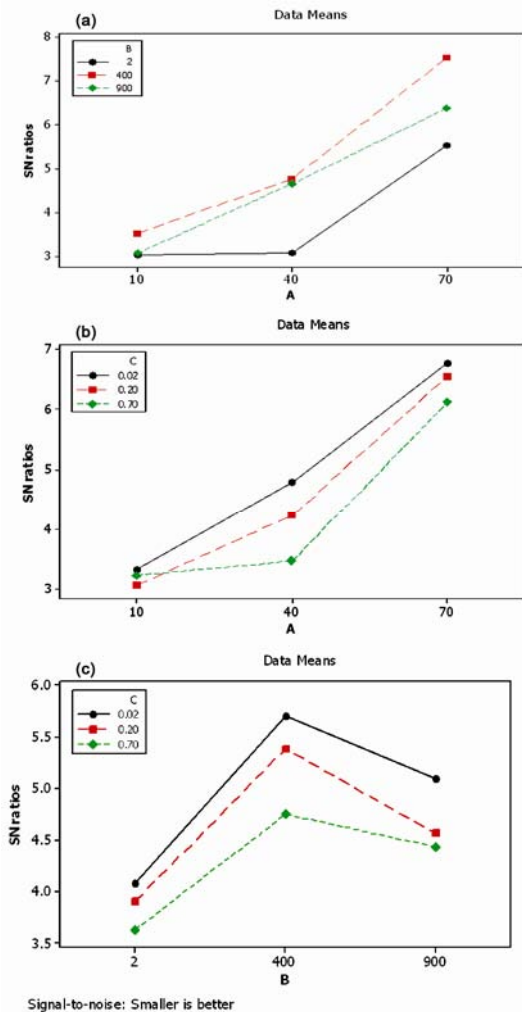


Fig. 5(a) — Interaction graph for AxB for COF, (b) — Interaction graph for AxC for COF, (c) — Interaction graph for BxC for COF

specific wear rate of the composites. Analysis of these results leads to the conclusion that factors combination A₃, B₂, C₁, D₃ and E₂ give minimum coefficient of friction as shown in the Fig. 4. The interaction graphs are shown in Figs 5 (a- c). From these figures it is observed that the interaction AxB shows significant effect on the coefficient of friction. Similarly the combination of factors A₃, B₂, C₁, D₂ and E₂ gives minimum specific wear rate as shown in the Fig. 6. The interaction graphs for parameters of specific wear rate are shown in Figs 7 (a-c). It is observed that interaction AxB also has a significant effect on the specific wear rate.

ANOVA and effects of factors

It is done an ANOVA of the data with coefficient of friction and specific wear rate, with the objective of analyzing the influence of normal load (A), filler content (B), roughness (C), speed (D) and sliding distance (E) on the total variance of the results. In order to understand the impact of various control factors and interaction on the response of experimental data it is desirable to develop the analysis of variance (ANOVA) to find the significant factor as well as interactions. ANOVA allows analyzing the influence of each variable on the total variance of the results. Table 4(a) shows the results of ANOVA for the coefficient of friction and Table 5(a) shows the results of ANOVA for the specific wear rate. It can be observed from the ANOVA Table 4(a) for coefficient of friction that the (A) normal load (P=75.33%) and filler content (P=13.23%) the interaction between (AxB) normal load and filler content (P=4.44%) have greater influence on the coefficient of friction and hence these are physically and statistically highly significant. However roughness (P=3.13%), the interaction between normal load and roughness (AxC) (P=1.85%) have a lesser

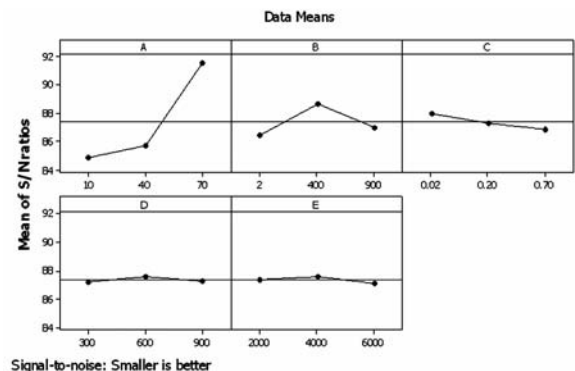


Fig. 6 — Main effect plot for S/N ratios for SWR

effect on the coefficient of friction as an error value (P=0.68%) is a small side hence less significant. From the analysis of ANOVA and response Table 4(b) of the S/N ratio of coefficient of friction, it is observed that the control parameter normal load has major impact on coefficient of friction followed by speed, sliding distance, roughness and filler contents. Under dry sliding conditions increasing applied normal load and sliding speed increases the temperature at the interface. This increase in temperature causes thermal penetration to occur, which results in weakness in bond at the filler-matrix interface. Consequently filler becomes the loose in the matrix and shear easily due to axial thrust. As a result coefficient of friction decreases. It was also found that the transfer film also

plays a very important role in affecting the friction and wear behaviour of vinylester composites¹⁵.

In the same way from the ANOVA Table 5(a) for the specific wear rate it is observed that the load (P=83.58%), filler content (P=8.39%) and roughness (P=1.83%). The interaction between (A×B) load and speed (P=3.87%) have great influence on the specific wear rate and hence these are physically and statistically highly significant. However, the interactions (B×C) between filler content and roughness (P=0.97%) have a lesser effect on specific wear rate as an error value (P=0.50%). From the analysis of ANOVA and response Table 5(b) of the S/N ratio for

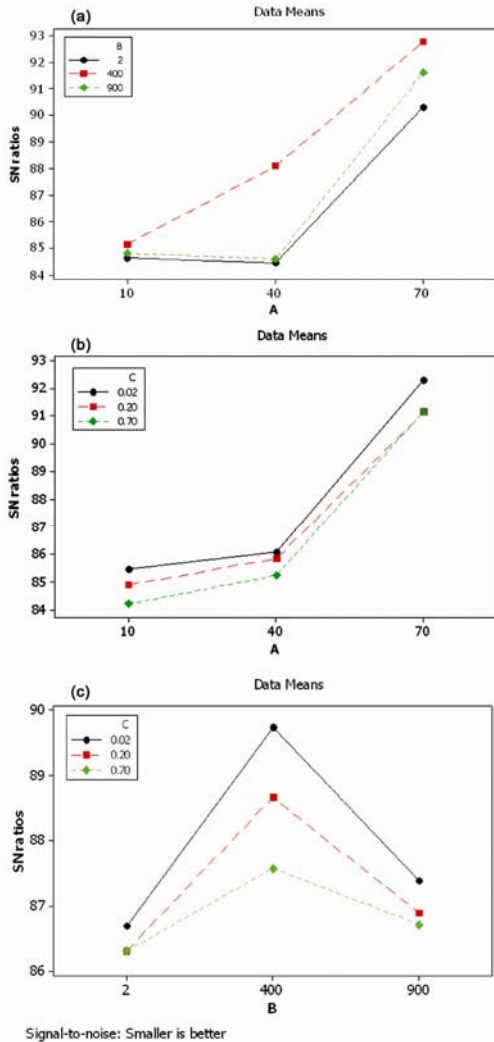


Fig. 7(a) — Interaction graph for AxB for SWR, (b) — Interaction graph for AxC for SWR, (c) — Interaction graph for BxC for SWR

Table 4 (a) — Analysis of variance for S/N ratios for coefficient of friction

Source	DOF	Seq SS	Adj MS	F	P (%)
A	2	51.162	25.58	219.2	75.33
B	2	8.989	4.494	38.52	13.23
C	2	2.128	1.064	9.12	3.13
D	2	0.338	0.169	1.45	0.49
E	2	0.221	0.110	0.95	0.32
A*B	4	3.021	0.756	6.48	4.44
A*C	4	1.260	0.315	2.70	1.85
B*C	4	0.325	0.081	0.70	0.47
Residual	4	0.466	0.116		0.68
Error	26	67.917			
Total					

Table 4(b) – Response table for S/N ratios for coefficient of friction

Level	A	B	C	D	E
1	3.203	3.870	4.957	4.669	4.529
2	4.156	5.276	4.617	4.459	4.740
3	6.481	4.697	4.269	4.716	4.574
Delta	3.278	1.406	0.688	0.258	0.211
Rank	1	2	3	4	5

Table 5(a) — ANOVA Analysis of variance for S/N ratios for specific wear rate

Source	DOF	Seq SS	Adj MS	F	P (%)
A	2	238.92	119.46	329.66	83.58
B	2	24.003	12.002	33.12	8.39
C	2	5.255	2.627	7.25	1.83
D	2	0.662	0.331	0.91	0.23
E	2	0.828	0.414	1.14	0.29
A*B	4	11.097	2.774	7.66	3.87
A*C	4	0.845	0.211	0.58	0.29
B*C	4	2.790	0.698	1.93	0.97
Residual	4	1.450	0.362		0.50
Error	26	285.85			
Total					

Table 5(b) — Response table for S/N ratios for specific wear rate

Level	A	B	C	D	E
1	84.85	86.44	87.94	87.23	87.40
2	85.70	88.66	87.29	87.58	87.56
3	91.54	87.00	86.87	87.27	87.14
Delta	6.69	2.22	1.07	0.35	0.43
Rank	1	2	3	5	4

specific wear rate, it is observed that the load has major impact on specific wear rate followed by speed, filler content, sliding distance and roughness. The cenosphere fillers with submicron size (400 nm) seemed to be more effective in reduction of the specific wear rate under both 10 N and 70 N of applied normal load. It can be concluded that the submicron sized reinforced composites have better tribological properties at higher load. At higher loads the polishing action of submicron particles can be strengthened which reduces the scuffing of the composites. The transfer films on the counterpart surface may be of higher quality at higher load compare to that formed at applied normal load¹⁵.

Morphology of worn surface

The SEM investigation has demonstrated the state of dispersion and distribution of the cenosphere at the micro structure level. The optical microscopy examinations of the worn surface of vinylester composites C₁, C₂ and C₃ against steel discs dry sliding conditions under applied load of 70 N and 900 rpm speed are shown in Figs 8(a-c). The SEM observation on Fig. 8(a) for vinylester samples (C₁) show that conditions matrix is uniformly spread over the specimen surface, cracks in the matrix and less wear debris can be seen that indicates higher wear rate. As observed from the figure it exhibit highest wear among all applied loads due to cutting mode of adhesive wear is occurring which results in deep grooves that are clearly visible in the micrograph. The disc worn surfaces of vinylester composite (C₁) show that more of the cenosphere exposures indicating higher wear rate. The composites C₂ and C₃ show the lesser spread of the matrix debris compare to C₁ composites under 70 N load and 900 rpm higher speed. From Fig. 8(b) for composite samples (C₂) the observations show that conditions the matrix is uniformly spread over a major portion of the specimen in the matrix that indicates lower wear rate. It was found that for the composites containing the larger (i.e. 2 μm and 900 nm) cenosphere, debonding cracks were formed in the interfacial regions between the particles and the matrix. However, debonding cracks were absent in the composites filled with 400 nm cenosphere particles. Instead, the networks of minute cracks were observed on the wear groove surface. A wear track is clearly visible in the micrograph. Close inspection of the debris revealed that some cenosphere particles were trapped inside the

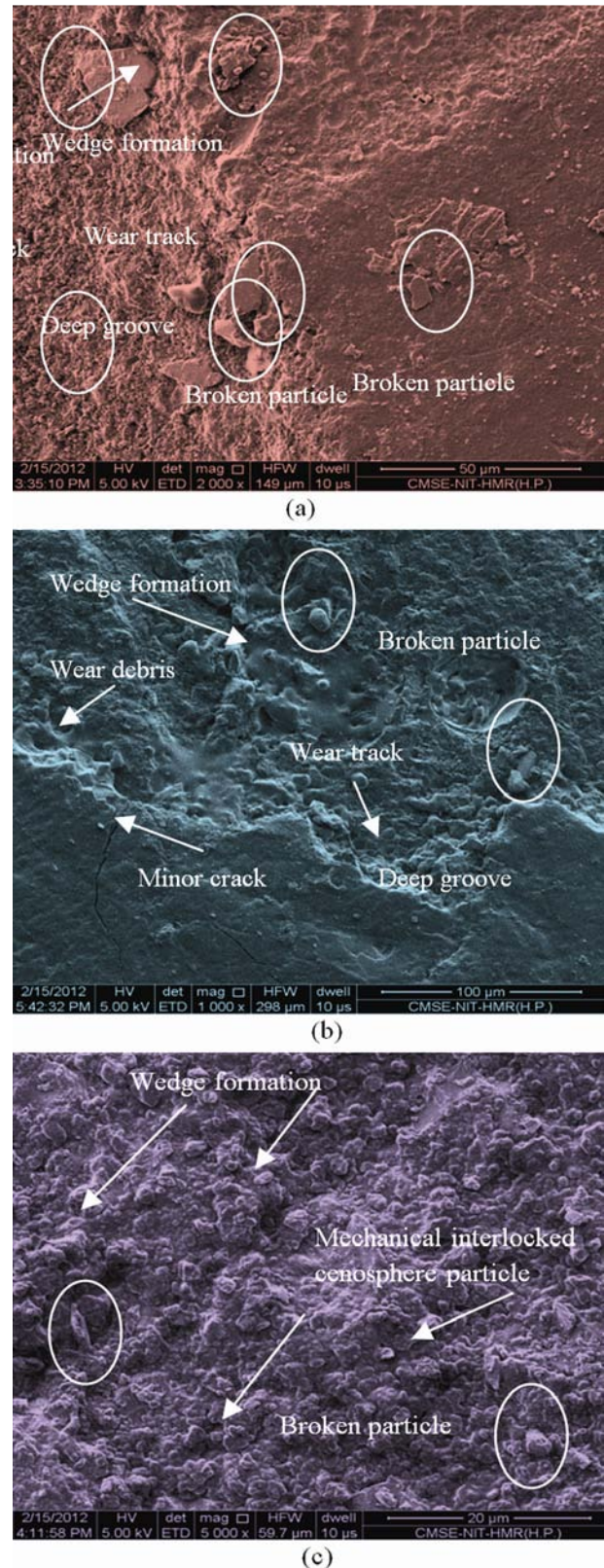


Fig. 8 — SEM micrograph of worn surface on specimen at load 70 N and speed 900 rpm (a) C₁, (b) C₂ and (c) C₃

removed vinylester. The examination of the wear scars indicated that the damage morphologies for all samples were similar.

Confirmation experiments

The confirmation experiment is the final step in the design of experiment process. The confirmation experiment is conducted to validate the inference drawn during the analysis phase. The confirmation experiment is performed by considering the new set of factor settings $A_3 B_2 C_1 D_3$ and E_2 to predict the coefficient of friction and for specific wear rate factor setting is $A_3 B_2 C_1 D_2 E_2$. The estimated S/N ratio for coefficient of friction can be calculated with the help of following predictive equation:

$$\eta_1 = \bar{T} + (\bar{A}_3 - \bar{T}) + (\bar{B}_2 - \bar{T}) + [(\bar{A}_3 \bar{B}_2 - \bar{T}) - (\bar{A}_3 - \bar{T}) - (\bar{B}_2 - \bar{T})] + (\bar{C}_1 - \bar{T}) + (\bar{D}_3 - \bar{T}) + (\bar{E}_2 - \bar{T}) \quad \dots (4)$$

Where η is the predicted average, T is average results of 27 runs and $A_3 B_2 C_1 D_3$ and E_2 is the mean response for factors and interactions at designated levels. By combining all the terms Eq. (4) reduces to:

$$\eta_1 = \bar{A}_3 B_2 + (\bar{C}_1 - \bar{T}) + (\bar{D}_3 - \bar{T}) + (\bar{E}_2 - \bar{T}) \quad \dots (5)$$

A new combination of factor levels $A_3 B_2 C_1 D_3$ and E_2 are used to predict the S/N ratio of the coefficient of friction through the predictive equation and is found to be $\eta_1 = 5.1840$. For each of performance measures an experiment is conducted for different combinations of factors and results are compared with those obtained from the predictive equation as shown in Table 6(a).

Similarly a prediction equation is developed for estimating S/N ratio of specific wear rate as given by the equation:

$$\eta_2 = \bar{T} + (\bar{A}_3 - \bar{T}) + (\bar{B}_2 - \bar{T}) + [(\bar{A}_3 \bar{B}_2 - \bar{T}) - (\bar{A}_3 - \bar{T}) - (\bar{B}_2 - \bar{T})] + (\bar{C}_1 - \bar{T}) + (\bar{D}_2 - \bar{T}) + (\bar{E}_2 - \bar{T}) \quad \dots (6)$$

Where η is the predicted average, T is average results of 27 runs and $A_3 B_2 C_1 D_2$ and E_2 is the mean response to factors and interactions at designated levels. By combining all the terms Eq. (6) reduces to:

$$\eta_2 = \bar{A}_3 B_2 + (\bar{C}_1 - \bar{T}) + (\bar{D}_2 - \bar{T}) + (\bar{E}_2 - \bar{T}) \quad \dots (7)$$

A new combination of factor levels $A_3 B_2 C_1 D_2$ and E_2 are used to predict the S/N ratio of specific wear rate

through the predictive equation and is found to be $\eta_1 = 93.7397$. For each of performance measures an experiment is conducted in different combinations of factors and results are compared with those obtained from the predictive equation as shown in Table 6(b). The resulting equations seem to be capable of predicting the coefficient of friction and specific wear rate to the acceptable level of accuracy. An error of 1.65 for the S/N ratio of the coefficient of friction and 2.46 for the S/N ratio of the specific wear rate is observed. However, if the number of observations of performance characteristics are increased further these errors can be reduced. This validates the statistical approach used for predicting the measures of performance based on knowledge of the input parameters.

Conclusions

Following conclusions can be drawn based on the experimental results of this study:

- (i) Design of experiments approach by Taguchi method enabled successfully to analyze the friction and wear behavior of the composites with normal load, speed, sliding distance and filler content as test variables.
- (ii) The experimental results show that the load and filler content are the main parameters among the five controllable factors (load, speed, sliding distance, roughness, filler content) that the influence coefficient of friction and specific wear rate.
- (iii) The effects of uniform sized submicron spherical cenosphere particles on the wear behaviour of vinylester composites were studied. The submicron particles and micro particles are both able to improve the wear resistance of the vinylester composites. The particle diameters used were 400 nm, 900 nm and 2 μ m, respectively. The submicron sized particles seemed to be more effective in improving the wear resistance as compared to that the micro sized particles.
- (iv) The tensile strength and compressive strength of the vinylester composites were significantly enhanced by filling with small size particles. The small size particle composite having great mechanical properties as compared to the large size particle composite. It is noticed that the hardness, flexural strength and compressive strength is increased linearly with decrease the particle size vinylester composite.

- (v) The experimental results show that load and filler content have percentage contribution 75.33% and 13.23% for coefficient of friction respectively.
- (vi) In the case of specific wear rate the applied normal load is significant parameter statistically as compared to other parameters. The percentage contribution of filler content is 83.58%.

References

- 1 Fried J R, *Polymer science and technology* (Prentice Hall, Upper Sadle River, New Jersey), 4, 1995.
- 2 Hollaway L, *Handbook of Polymer Composites for Engineers*, 1st ed (Jaico Publishing House, Mumbai), 1995, 24-28: 73-76.
- 3 Feng S, Zhang Z & Liu W, *Wear*, 260 (2006) 861-868.
- 4 Zsidai L, Baets P, Samyan P & Kalacska G, *Wear*, 253 (2002) 673-688.
- 5 Jia J H, Zhou H D, Gao S Q, & Chen J M, *Mater Sci Eng*, 356 (2003) 48-53.
- 6 Bolvari A E & Gleen S B, *Eng Plast*, 9 (3) (1996) 205-215.
- 7 Hongwei H, Kaixi L, Jain S, Yanqui L & Jianlong W, *Mater Des*, 32 (2011) 4521-4527.
- 8 Velde F & Bakats P, *Wear*, 209 (1997) 106-114.
- 9 Hutchings I M, *Tribology Friction and Wear of Engineering Materials* (London, CRC, Press), 1992.
- 10 Chauhan S, Kumar A, Patnaik A, Satapathy A & Singh I, *J Reinf Plast Compos*, 28 (2009) 2675-2684.
- 11 Unal H, Mimaroglu, Kadioglu U & Ekiz H, *Mater Des*, 5 (2004) 239-245.
- 12 Friedrich K, Lu Z & Hager A M, *Wear*, 190 (1995) 139-144.
- 13 hang N, Chan Li Xi, Yin Y S, Han Ye & Wang Z F, *Mater Sci Forum*, 686 401-405. doi:10.4028/MSF.686.401.
- 14 Yeh H Y & Yang S C, *J Reinf Plast Compos*, 16(5) (1997) 414-418.
- 15 Xing X S & Li R K, *Wear*, 256 (2004) 21-26.
- 16 Xian G, Walter R & Hauptert F, *Compos Sci Technol*, 66 (2006) 3199-3209.
- 17 Yu S, Hu H, Ma J & Yin J, *Tribol Int*, 41 (2008)1205-1211.
- 18 Scott W D, Heldt T, Van Erp G & Ayers S R, *FRP Int*, 2 (2005) 2-5.
- 19 Singh B P, Jain R C & Bharadwaj I S, *J Polym Sci*, 2 (1994) 941.
- 20 Chauhan S R, Kumar Anoop & Singh I, *J Mater Sci*, 44 (2009) 6338-6347.
- 21 Rong M Z, Zhang M Q, Liu H & Zeng H M, *Lub Tribol*, 53 (2) (2001) 72-77.
- 22 Lin J C, *Compos Pt B – Eng*, 38 (2007) 79-85
- 23 Ross P J, *Taguchi technique for quality engineering* (Mc Graw-Hill, New York), 1993, 1-40.
- 24 Roy K R, *A primer on Taguchi method* (Van Nostrad reinhold, New York) 1990.
- 25 Chauhan S R, Anoop Kumar, Singh I & Kumar Prashant, *J MinerMater Charact & Eng*, 9 (4) (2010) 365-387.
- 26 Taguchi G, *Taguchi on robust technology development methods* (ASME press, New York), 1993, 1-40.
- 27 Glen S P, *Methods Taguchi*, (A hands on approach. NY: Addison-Wesley), 1993.